Cancer Cell
Article

Suppression of Colon Cancer Metastasis by Aes through Inhibition of Notch Signaling

Masahiro Sonoshita,[1,7] Masahiro Aoki,[1,7,9] Haruhiko Fuwa,[2] Koji Aoki,[1] Hisahiro Hosogi,[1,3] Yoshiharu Sakai,[3] Hiroki Hashida,[4] Arimichi Takabayashi,[4] Makoto Sasaki,[2] Sylvie Robine,[5] Kazuyuki Itoh,[6] Kiyoko Yoshioka,[6] Fumihiko Kakizaki,[1] Takanori Kitamura,[1] Masanobu Oshima,[1,8] and Makoto Mark Taketo[1,*]
[1]Department of Pharmacology, Graduate School of Medicine, Kyoto University, Kyoto 606-8501, Japan
[2]Laboratory of Biostructural Chemistry, Graduate School of Life Sciences, Tohoku University, Sendai 981-8555, Japan
[3]Department of Surgery, Graduate School of Medicine, Kyoto University, Kyoto 606-8501, Japan
[4]Department of Gastroenterological Surgery and Oncology, Kitano Hospital, Osaka 530-8480, Japan
[5]Equipe de Morphogenèse et Signalisation cellulaires, Institut Curie, 75248 Paris, France
[6]Department of Biology, Osaka Medical Center for Cancer and Cardiovascular Diseases, Osaka 537-8511, Japan
[7]These authors contributed equally to this work
[8]Present address: Division of Genetics, Center for Cancer and Stem Cell Research, Kanazawa University, Kanazawa 920-0934, Japan
[9]Division of Molecular Pathology, Aichi Cancer Center Research Institute, Nagoya 464-8681, Japan
*Correspondence: taketo@mfour.med.kyoto-u.ac.jp
DOI 10.1016/j.ccr.2010.11.008

SUMMARY

Metastasis is responsible for most cancer deaths. Here, we show that *Aes* (or *Grg5*) gene functions as an endogenous metastasis suppressor. Expression of Aes was decreased in liver metastases compared with primary colon tumors in both mice and humans. Aes inhibited Notch signaling by converting active Rbpj transcription complexes into repression complexes on insoluble nuclear matrix. In tumor cells, Notch signaling was triggered by ligands on adjoining blood vessels, and stimulated transendothelial migration. Genetic depletion of *Aes* in $Apc^{\Delta 716}$ intestinal polyposis mice caused marked tumor invasion and intravasation that were suppressed by Notch signaling inhibition. These results suggest that inhibition of Notch signaling can be a promising strategy for prevention and treatment of colon cancer metastasis.

INTRODUCTION

Most cancer patients die of metastasis. Although there have been substantial advances in our understanding of the mechanisms of cancer metastasis, efficient remedies for prevention and treatment of metastasis are still missing. The invasion-metastasis cascade consists of local invasion, intravasation, transport, extravasation, formation of micrometastases, and colonization (Fidler, 2003; Steeg, 2006). This sequence is completed only infrequently, causing metastatic inefficiency, and the least efficient of these steps appears to be colonization (Smith and Theodorescu, 2009). Spread of metastatic cancer cells via blood circulation is responsible for the majority of distant metastases, although they may travel also through the lymph ducts to nodes (Weinberg, 2007). In colorectal cancer, metastatic tropism to the liver and lungs can be explained largely by the organization of venous circulation of the intestines through portal vein to the liver, and further to the lungs through pulmonary artery.

Among endogenous colon tumor models, the widely used *Apc* (*Adenomatous polyposis coli*) mutant mice form adenomas in the small intestine, with wide multiplicities (3−300 per animal) depending on the mutational allele, although several adenomas are also found in the colon (Taketo and Edelman, 2009). Additional mutations introduced into *Apc* mutant mice can modify the tumor phenotype. For example, knocking out *Smad4* gene in the TGF-β family signaling converts the benign intestinal adenomas to very invasive adenocarcinomas (Takaku et al.,

Significance

We have found that Aes suppresses colon cancer metastasis by inhibiting Notch signaling pathway. The molecular mechanism of Notch inhibition is through transcriptional repression by sequestering Rbpj, NICD, and Maml1 to nuclear matrix. The cellular mode of metastasis suppression includes inhibition of transendothelial migration (TEM) of tumor cells, which blocks intravasation. Heterotypic interaction between cancer and host cells activates Notch signaling and promotes TEM of metastasizing cancer cells. Because TEM in metastasis is common to many solid tumors, this mechanism is important in various types of cancers. As a model for colon cancer invasion and intravasation, compound mutant mice for the *Apc* and *Aes* genes should be useful to evaluate upcoming therapeutics including Notch signaling inhibitors against colon cancer metastasis.

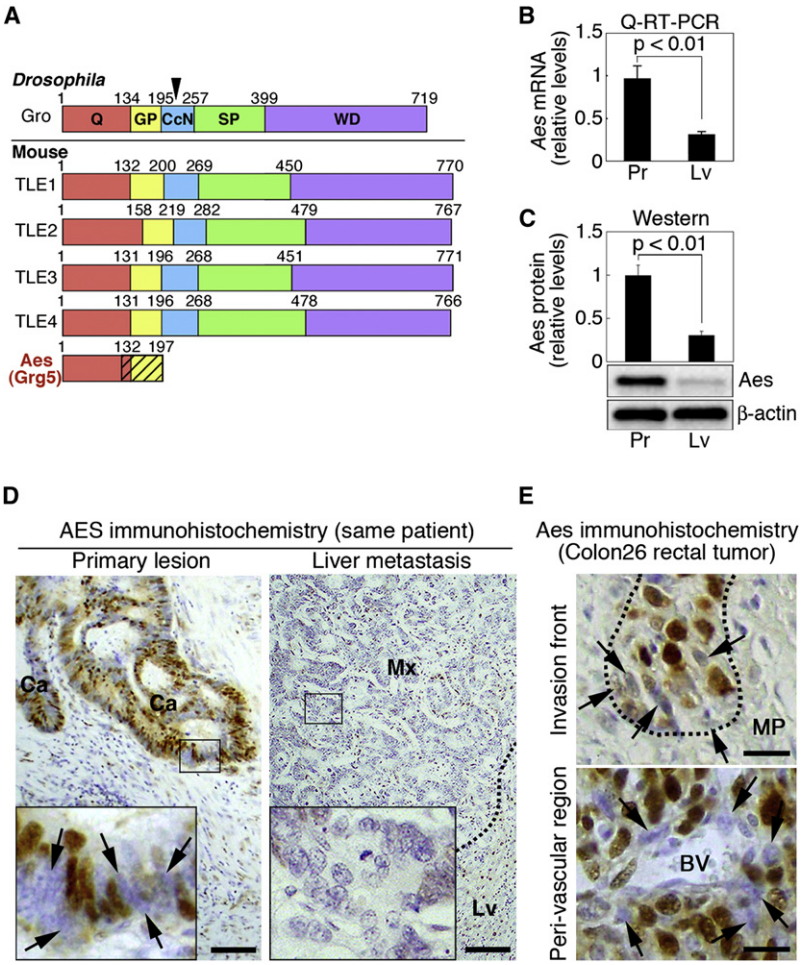

Figure 1. *Aes* as a Metastasis Suppressor Candidate

(A) Schematic representation of fly and mouse Gro/TLE family protein structures. Hatched region in Aes shows a limited identity with TLEs (~65%). Q, glutamine-rich domain (orange); GP, glycine-proline-rich domain (yellow); CcN, domain containing putative phosphorylation sites for cdc2 and casein kinase II (CK2) adjacent to nuclear localization signals (triangle) (blue); SP, serine-proline-rich domain (*green*); WD, domain containing series of tandem repeats of tryptophan and aspartic acid residues (purple). Numbers indicate amino acid residues.

(B) Expression levels of *Aes* mRNA in mouse Colon26 cells determined by quantitative (Q-)RT-PCR. Pr, primary tumors. Lv, liver metastases. Error bars indicate SD. (n = 3).

(C) Expression levels of Aes protein in Colon26 cells determined by western blotting. Same keys as in (B).

(D) Immunostaining for AES in a primary human colon cancer (left) and its liver metastasis (right) from the same patient. Boxed areas are shown in insets, respectively. Dotted line indicates the boundary between metastasis (Mx) and normal liver tissue (Lv). Note that some cancer cells at the invasive fronts had lost expression of *AES* (arrows). Ca, cancer epithelium. Scale bars, 100 μm. Nuclei were counterstained with hematoxylin.

(E) Loss of *Aes* expression on the invasive front of mouse Colon26 primary tumors (arrows). Dotted line indicates the boundary between invading cancer cells and host *muscularis propria* (MP). BV, blood vessel. Scale bars, 10 μm.

See also Figure S1.

1998). Even in such a model, the adenocarcinomas are only locally invasive, and neither intravasation nor distant metastasis is observed during the short life span of these mice. Accordingly, we have screened for candidate genes whose inactivation can stimulate metastasis of transplanted mouse colon cancer cells from the rectum to the liver, the commonest site of metastasis.

RESULTS

Aes as a Metastasis Suppressor Candidate

To identify genes responsible for metastasis suppression, we first prepared a syngeneic and orthotopic transplantation model of colon cancer metastasis in the mouse. When injected into the rectal smooth muscle layer, Colon26 cells can metastasize to the liver, lungs, and lymph nodes in the Balb/c hosts at different efficiencies (Corbett et al., 1975; Kashtan et al., 1992; Tsutsumi et al., 2001) (see Figures S1A–S1F available online). As a preliminary screening, we compared gene expression profiles between the primary tumors and their liver metastases using cDNA microarrays. While many genes showed differential expression, we focused on the category of "transcription regulator activity" in search for master regulators that control metastatic traits. Because cell migration and motility appear to be key traits of metastatic cancer (Christofori, 2006; Weinberg, 2007), we tested ~20 downregulated genes for inhibition of Colon26 invasion in vitro through Matrigel and found one that showed a strong activity, though it was at the 26th of the list (Figure S1G). This gene, *Amino-terminal enhancer of split* (*Aes*), also called *Grg5* in mice, is a member of the *Groucho/Transducin-Like Enhancer of split* (*Gro/TLE*) gene family, with its Q/GP domains showing similarities to those in TLEs (Gasperowicz and Otto, 2005; Lepourcelet and Shivdasani, 2002; Brantjes et al., 2001) (Figure 1A). Although mouse *Aes* helps development of bone and the pituitary gland (Mallo et al., 1995; Brinkmeier et al., 2003), its role in cancer progression has not been investigated. Consistent with the microarray and Matrigel results, mouse *Aes* was significantly downregulated in the liver and lung metastases, upon determinations by quantitative (Q-) RT-PCR (Figure 1B) and western blots (Figure 1C). Importantly, human liver metastatic lesions in 29 out of 52 colon cancer patients (i.e., 56%) expressed significantly lower levels of AES protein than primary tumors from the same patients (Figure 1D). Curiously, some cancer cells had already lost expression of *AES/Aes* at the invasion fronts in both human (Figure 1D, inset in the left panel) and mouse (Figure 1E) colon primary tumors. Furthermore, absence of AES in human colon cancer significantly correlated with vascular invasion ($p < 0.01$), distant metastasis ($p = 0.01$) and progression stages ($p = 0.02$; $n = 83$).

To investigate the roles of *Aes* in colon cancer metastasis, we constructed Colon26 cell derivatives whose *Aes* expression was

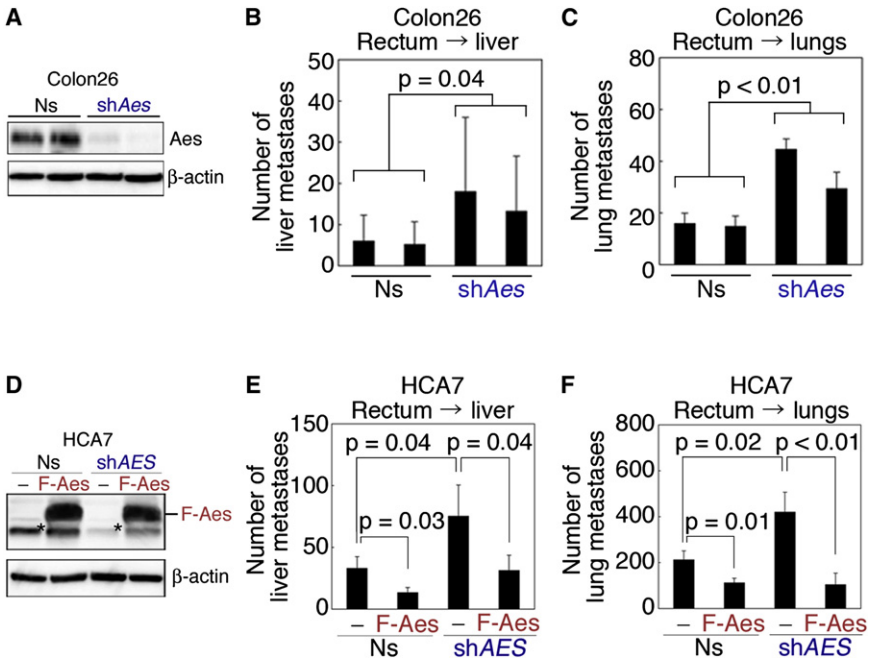

Figure 2. Suppression of Colon Cancer Metastasis by *Aes*

(A–C) Effects of *Aes* knockdown in mouse Colon26 cells (A) on their metastasis to the liver (B) and lungs (C), respectively. Multiple Colon26-derived clonal cell lines were isolated that expressed one of three different shRNA constructs, followed by the rectal transplantation. Data are shown for such cell lines derived from two distinct shRNA clones whose experiments were performed simultaneously, and similar data were obtained with a third clone (not shown). Ns, nonsilencing control. sh*Aes*, shRNA against *Aes* mRNA. Error bars indicate SD (n = 10).

(D–F) Effects of *Aes* overexpression in a human colon cancer cell line HCA7 (D) on its metastasis to nude mouse liver (E) and lungs (F) from the rectum, respectively. A clonal cell line expressing flag-tagged mouse Aes (F-Aes) was compared with a control containing the empty vector (–) (D); left half; Ns for nonsilencing control). The same set of cell lines were introduced with a construct that expressed an shRNA against human *AES* (sh*AES*; (D), right half). Asterisks show the band position for the endogenous human AES protein (western blot analysis). Note that metastasis-promoting effects of sh*AES* was suppressed by overexpression of mouse Aes (F-Aes), excluding the possibility of off-target effects by sh*AES*. Each data set shown is a representative of two. Error bars indicate SD (n = 5).

See also Figure S2.

knocked down constitutively by shRNA constructs (sh*Aes*) (Figure 2A). As anticipated, *Aes* knockdown promoted Colon26 metastasis from the Balb/c mouse rectum to liver (Figure 2B) and lungs (Figure 2C), for all clones derived from three independent shRNAs. Likewise, knockdown of human *AES* (Figure 2D) increased the number of metastases for HCA7 human colon cancer cells (Kirkland, 1985) to both liver (Figure 2E) and lungs (Figure 2F) of nude mice. Convincingly, this knockdown effect was reversed by overexpression of flag-tagged mouse *Aes* (F-Aes) that was not targeted by the shRNA against human *AES* (Figures 2D–2F). We then constitutively overexpressed *Aes* in Colon26 cells at the level five times higher than that of endogenous *Aes*, injected them into the mouse rectum, and found that their metastasis was suppressed significantly to both liver and lungs (Figures S2A–S2D). Notably, *Aes* suppressed lung metastasis of the cancer cells also upon intravenous injections (Figure S2E), another model of hematogenous metastasis that bypasses local invasion and intravasation (Price, 2001). Importantly, neither knockdown nor overexpression of *Aes* affected the size of primary tumors (Figures S2F–S2H). These results indicate that *Aes* suppresses colon cancer metastasis without affecting the growth of primary tumors.

Aes Is an Endogenous Notch Signaling Inhibitor

In colonic tumor formation and its malignant progression, Wnt, TGF-β, Hedgehog, and Notch signaling pathways appear to play key roles (Sancho et al., 2004; van Es et al., 2005; Taketo, 2006; Takaku et al., 1998), not to mention KRAS and p53. Interestingly, Gro/TLE cotranscription factors have been implicated in some of these pathways (Roose et al., 1998; Chen and Courey, 2000; Wang et al., 2002). We first investigated the possible role of Aes in Wnt signaling because of its Q and GP domains similar to those in TLE proteins that can inhibit the signaling (Brantjes et al., 2001). Although we confirmed repression by TLE1 to ~20%, Aes had only marginal effects on LEF1/β-catenin-induced TOPFLASH activation in HEK293 human embryonic kidney cells (Figure S3A). Aes also failed to suppress Wnt signaling in Colon26 cells (Figure S3B, left).

We then assessed the effects of Aes on other signaling pathways in colon cancer cells by transactivation assays using established luciferase reporters. Aes did not affect TGF-β or Hedgehog pathways (Figure S3B, center or right). Instead, Aes significantly inhibited Notch signaling, a critical signaling in development (Artavanis-Tsakonas et al., 1999; Hurlbut et al., 2007; Ilagan and Kopan, 2007), as determined by pGa981-6 reporter containing Rbpj (Recombination signal binding protein of the Jκ immunoglobulin gene, or CSL; CBF1 in human)-binding sites and a luciferase gene (Kato et al., 1997). Namely, expression of exogenously introduced *Aes* dose-dependently repressed both endogenous and RAMIC (Rbpj-associated molecule domain and intracellular domain of the Notch receptor, a recombinant protein equivalent to NICD, Notch intracellular domain) (Kato et al., 1997)-induced transcription of the reporter in Colon26 cells (Figure 3A). Of note, 293T cells showed the strongest activity of endogenous Notch signaling among 30 cell lines analyzed, and Aes caused tighter repression in these cells (to ~20%) (Figure S3C). Consistently, induction of Aes by doxycycline in Colon26 TetONF-Aes cells suppressed expression of endogenous Notch target *Hes1* (Figure S3D). On the other hand, knockdown of *Aes* doubled the activity of both the

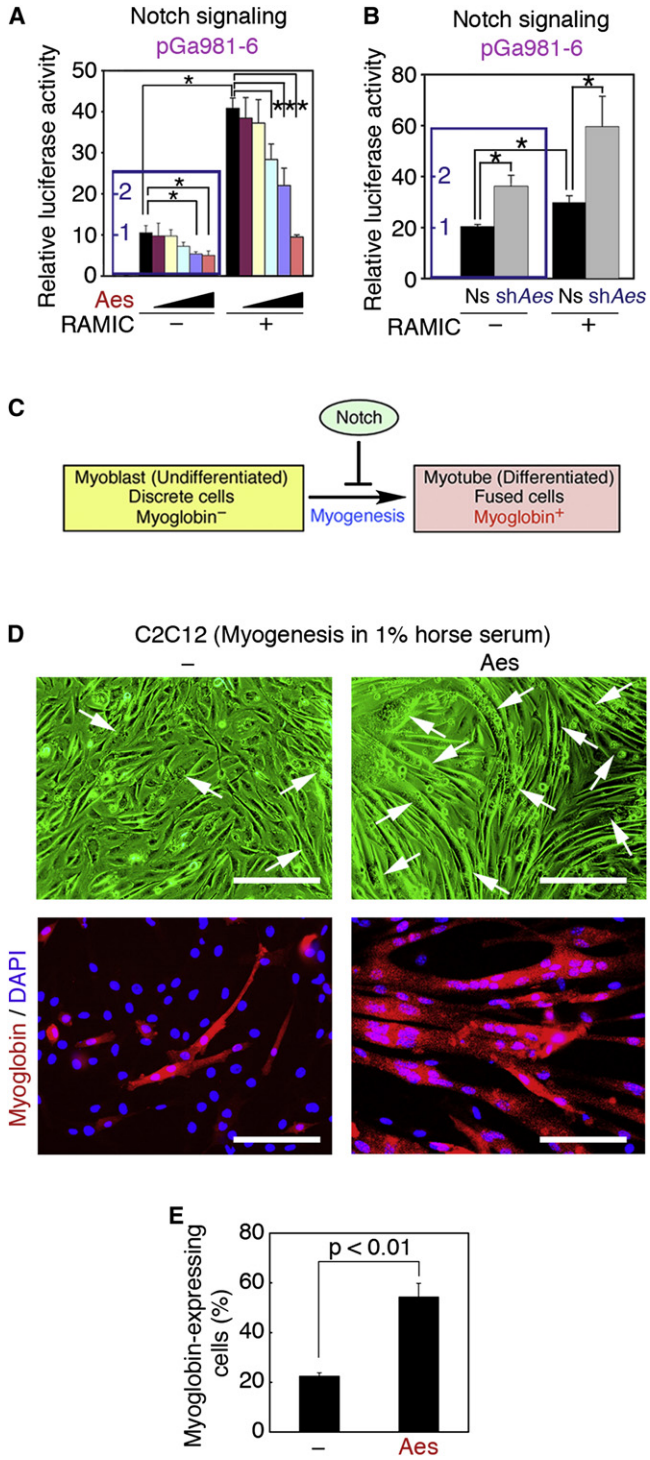

Figure 3. Inhibition of Notch Signaling by *Aes*

(A and B) Effects of *Aes* overexpression (A) and *Aes* knockdown (B) on Notch signaling in Colon26 cells determined by pGa981-6 luciferase reporter assay in the absence (–) or presence (+) of exogenously introduced RAMIC. Insets (blue frames) show the endogenous reporter activities. Ns, nonsilencing control. *$p < 0.01$ compared with the controls. Error bars indicate SD (n = 3).

(C) A schematic representation of the role of Notch signaling in myogenesis.

(D) Effects of Aes on myoblast differentiation. Rat C2C12 myoblasts were transfected with either the vector or Aes cDNA, and three stable clones were isolated, respectively. Myogenesis was induced by a medium containing 1% horse serum for 4 days. Myoglobin, a myotube marker, was immunostained (red) in C2C12 clones with or without overexpressed Aes. Nuclear DNA was stained with DAPI (blue). Arrows, myotubes with multiple nuclei. Scale bars, 100 μm.

(E) Quantification of the myoglobin-expressing cells in (D). Error bars indicate SD (n = 3).

See also Figure S3.

endogenous and RAMIC-induced Notch signaling in Colon26 cells (Figure 3B). Consistent with these data, *Aes* enhanced myogenic differentiation of C2C12 myoblasts in a representative biological assay for Notch signal inhibition (Kato et al., 1997) (Figures 3C–3E).

Because Aes and TLE proteins shared structural similarities (Figure 1A), we next asked whether TLE1 also inhibited Notch signaling. In contrast to Aes, TLE1 failed to repress the RAMIC-induced transactivation in 293T cells, human colon cancer HCT116 cells, and mouse Colon26 cells (Figure 4A; data not shown). Interestingly, however, coexpression with TLE1 significantly potentiated the repression by Aes. It was reported that Aes interacted with TLE1 in yeast (Pinto and Lobe, 1996), and we found coprecipitation of endogenous Aes and TLE1 in the lysates of colonic tumors from $Apc^{\Delta 716}$ mice (Oshima et al., 1995) (Figure 4B). Notably, we found nuclear colocalization of Aes and TLE1 forming distinct foci in $Apc^{\Delta 716}$ adenoma cells (Figure 4C). We further studied subcellular localization of Aes in cultured cells. When transfected alone, Aes fused to *Aequorea coerulescens* GFP (AcGFP-Aes) showed diffuse distribution in both the cytoplasm and nucleoplasm of live HCT116 cells (Figure 4D). Intriguingly, coexpression with TLE1 caused dramatic relocation of AcGFP-Aes to nuclei, causing distinct foci (Figure 4D). Similar results were obtained with 293T and Colon26 cells (data not shown).

We next employed deconvolution microscopy, and analyzed subnuclear localization of the Notch effectors; Rbpj, RAMIC (NICD), and Maml1 (Mastermind-like 1). In the absence of Aes/TLE1 complex, Rbpj, RAMIC, and Maml1 all showed diffuse nucleoplasmic distribution in HCT116 cells. When cotransfected with Aes and TLE1, however, RAMIC and Maml1 relocated to nuclear foci that also contained Aes and TLE1, whereas Rbpj distributed both in the foci and the nucleoplasm (Figures 4E and 4F).

To determine the roles of these nuclear foci in transcription, we performed in situ transcription labeling, and visualized BrUTP incorporation into mRNA during 5 min prior to fixation. When Notch effectors were coexpressed with Aes and TLE1, BrUTP uptake into mRNA was scarce in the nuclear foci where Maml1 resided (Figure 4G). These foci were not stained with anti-PML, anti-SC35, or anti-fibrillarin antibody, suggesting that they are distinct from PML bodies, RNA splicing bodies, and nucleoli (Zimber et al., 2004) (data not shown). Rather, lack of transcription in the foci was reminiscent of Bach2 foci, the nuclear bodies containing HDAC4 (Histone deacetylase 4) and SMRT (Silencing mediator of retinoid and thyroid receptor), and possibly related to matrix-associated deacetylase (MAD) bodies (Downes et al., 2000; Hoshino et al., 2007). In situ nuclear matrix preparation revealed that the Aes nuclear foci were indeed in the insoluble nuclear matrix fraction (Figure 4H). Moreover, HDAC3 was

associated and colocalized with Aes in the nuclear foci (Figure S4). Collectively, these results suggest that Aes, together with TLE1, can hold the Rbpj/NICD/Maml1 complex in nuclear foci where transcription is repressed.

Notch Signaling Inhibition Can Suppress Metastasis

Above results also suggested that *Aes* suppressed metastasis through inhibition of Notch signaling. As anticipated, attenuation of the signaling by constitutive expression of shRNA constructs against *RBPJ* mRNA (sh*RBPJ*) suppressed metastasis of HCA7 human colon cancer cells from the rectum to liver (multiplicity; 6.0 ± 2.7 versus 2.6 ± 1.6, $p = 0.02$) and to lungs (341 ± 89 versus 87 ± 40, $p < 0.01$) (Figures 5A and 5B) in nude mice. We obtained similar results also with mouse Colon26 cells expressing a dominant-negative mutant of Rbpj (dnRbpj; R218H; Kato et al., 1997) (Figures S5A and S5B). We then tested inhibition of Notch signaling with Compound E, a potent γ-secretase inhibitor (Milano et al., 2004; Schmidt, 2003; Zaczek et al., 1999) (GSI) (Figure 5C). It significantly suppressed metastasis of Colon26 cells to the liver (5.7 ± 5.5 versus 1.8 ± 2.4, $p = 0.04$) and lungs (54 ± 22 versus 18 ± 8, $p < 0.01$) (Figure 5D) from the rectum. Importantly, none of sh*RBPJ*, dnRbpj, or Compound E affected the size of primary tumors significantly (Figures S5C–S5E). Likewise, Compound E had little effect on the primary Colon26 tumors regarding their differentiation and proliferation (Figures S5F and S5G). These results underscore that Notch signaling plays an essential role in hematogenous metastasis of colon cancer cells.

Notch Activation by Stromal Ligands Induces Tumor Intravasation

Using immunofluorescence staining, we found that mouse Colon26 cells expressed abundant Notch1 receptor (Figure 6A, left), consistent with a report on human colon cancer (Zagouras et al., 1995). Notably, there was much Jagged1 ligand on the blood vessels in primary tumors (Figure 6A) as well as in their metastases to the liver (Figure 6B) and lungs (Figure 6C, left). Jagged1 was expressed also on normal epithelial cells in these organs (Figure 6B, Lv; hepatocytes: Figure 6C, right, Lg; pneumocytes expressing TTF-1). We also found that blood vessels and macrophages expressed another Notch ligand Delta-like 4 (Dll4) (Figures S6A–S6C). Curiously, activated NICD was detected in the tumor epithelium that was surrounded by DLL4-expressing stromal cells in human colon cancer tissues (Figure 6D). We employed the Q scoring (Detre et al., 1995), and obtained Spearman's correlation factor of 0.69, indicating a very strong association (0.6–0.8) between DLL4 and NICD expression ($p < 0.01$).

To test whether ligand-expressing stromal cells activated Notch signaling in cancer cells, we constructed "Notch reporter Colon26 ($C26^{RBS\text{-}EGFP}$) cells" that contained RBS (Rbpj binding sequence)-EGFP reporter, expressing EGFP upon Notch signal activation (Figure 6E). As expected, expression of RAMIC induced EGFP in the reporter cells in culture (Figure 6F). Convincingly, the EGFP staining was strongest in the $C26^{RBS\text{-}EGFP}$ cells located around blood vessels of the primary tumor in the Balb/c rectum (Figure 6G, left). Treatment of the tumor-bearing mice with Compound E, as well as overexpression of Aes in the reporter cells, almost eliminated expression of EGFP (Figure 6G, center and right), supporting that Aes acts through suppression of the Notch signaling. Interestingly, we found expression of EGFP in two types of metastasized cell clusters in the lung; micrometastases consisting of only a few cancer cells (Figure 6H, left), and cells at the periphery of larger metastases that were expanding in the lung parenchyma (Figure 6H, right) (see Discussion).

Because *Aes* was downregulated in cancer cells adjoining blood vessels (Figure 1E, bottom), we hypothesized that loss of *Aes* expression stimulated transendothelial migration (TEM) through Notch signal activation. To test the hypothesis in vitro, we placed cancer cells on a layer of HUVEC (human umbilical vein endothelial cells) that expressed Notch ligands (Lu et al., 2007; Mailhos et al., 2001). As expected, knocking down *Aes* in Colon26 cells stimulated HUVEC-induced Notch signaling as determined by Q-RT-PCR of *Hes1* mRNA (Figure 6I) and enhanced their TEM through the HUVEC layer (Figure 6J). Similar results were obtained with HCA7 cells (Figure S6D). Notably, expression of sh*RBPJ*s inhibited Notch signaling that was triggered by HUVEC (Figure 6K) and reduced their TEM significantly (Figure 6L). To observe TEM more dynamically, we took time-lapse movies of Colon26 cells with or without Aes induction migrating through the HUVEC cell layer (Movie S1). While approximately two-thirds of control Colon26 cells migrated underneath the HUVEC layer in 12 hr, only approximately one-third of the Aes-overexpressing Colon26 cells did (Figure S6E). We also found that recombinant DLL4 and JAGGED1 activated Notch signaling and enhanced motility of Colon26 cells when analyzed by simpler scratch assays (Figure S6F). These results are consistent with our hypothesis that *Aes* suppresses metastasis of colon cancer cells by inhibition of Notch signaling that stimulates cancer cell motility and TEM at the steps of local invasion, intravasation, and extravasation (see Discussion).

Aes Knockout Causes Tumor Intravasation

To test above hypothesis with endogenous tumors, we constructed a floxed allele of *Aes* (*Aes*^{f}), and introduced it into the *Apc*$^{\Delta 716}$ intestinal polyposis model carrying villin-Cre^{ERT2} transgene (*TgvCre*^{ERT2}) (el Marjou et al., 2004) whose tumors expressed substantial amounts of Aes (Figures 7A and 7B; Figures S7A and S7B). At 3 weeks of age, we treated the compound mutant *Apc*$^{+/\Delta 716}$-*Aes*$^{f/f}$-*TgvCre*^{ERT2} with 4-hydroxytamoxifen (4HT) to activate Cre recombinase in the intestinal epithelium, generating *Apc*$^{+/\Delta 716}$-*Aes*$^{\Delta ex2/\Delta ex2}$-*TgvCre*^{ERT2} genotype (*Apc*/*Aes*). In these mice that had lost *Aes* exon 2 (Figure S7C), we found marked tumor invasion and intravasation into the smooth muscle layer of the small intestine and colon (Figures 7D and 7E; *Apc*/*Aes*). Although all *Apc*/*Aes* mutants (25 examined) showed this invasion phenotype at 17 weeks of age, *Apc*$^{\Delta 716}$ polyposis mice never did (Kitamura et al., 2007; Oshima et al., 1995; Takaku et al., 1998) (Figure 7C; *Apc*). For the *Apc*/*Aes* polyps larger than 2 mm in diameter, about half of them was found invading into the submucosa or beyond (Figure 7F).

Strikingly, many of the invading tumor glands in the *Apc*/*Aes* mice were found inside vessels that were often distended, reminiscent of tumor embolism (Figure 7G, left). This intravasation was further confirmed by immunofluorescence for epithelial marker cytokeratin and vessel marker CD31 or blood vessel marker VE-cadherin (Figure 7G, center and right, respectively). Although such intravasating tumor epithelial cells should be

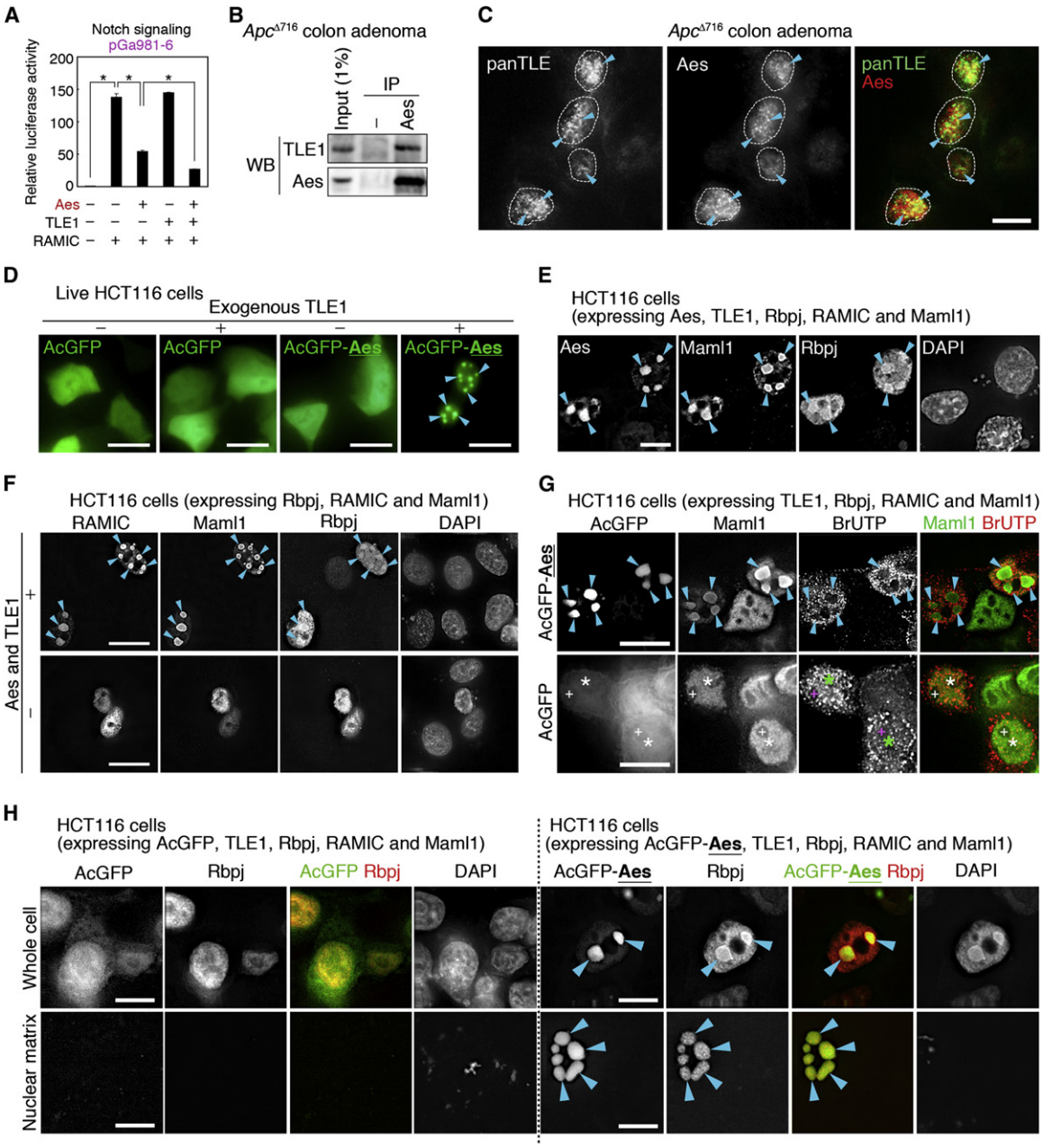

Figure 4. Colocalization of Aes and TLE1 with Notch Pathway Proteins in Nuclear Foci

(A) Effects of overexpression of Aes and TLE1 on RAMIC-induced Notch signaling determined by pGa981-6 luciferase reporter in HEK293 cells. *$p < 0.01$. Error bars indicate SD ($n = 3$).

(B) In vivo interaction between endogenous Aes and TLE1 in colonic adenomas of *Apc*$^{\Delta 716}$ mice. Aes in the tumor lysates was immunoprecipitated (IP) using anti-Aes antibody. Subsequently, Aes and TLE1 in the precipitates were detected by western blotting (WB).

(C) Immunofluorescence of endogenous TLE and Aes in an *Apc*$^{\Delta 716}$ colon adenoma. TLE proteins were detected by anti-panTLE antibody that had been raised against WD repeats. Arrowheads indicate colocalization of TLE and Aes in the nucleus (circled by broken lines). Scale bar, 10 μm.

(D) Effects of TLE1 overexpression on localization of Aes. HCT116 cells were transfected with expression plasmids for AcGFP or AcGFP-Aes simultaneously with or without TLE1. Twenty-four hours after transfection, localization of AcGFP in live cells was analyzed under a fluorescent microscope. Scale bars, 10 μm.

(E) Immunofluorescence of overexpressed Aes, Maml1, and Rbpj in HCT116 cells. Note colocalization of Aes, Maml1, and Rbpj in nuclear foci (arrowheads). Scale bar, 10 μm.

(F) Immunofluorescence of overexpressed RAMIC, Maml1 and Rbpj in HCT116 cells. Note colocalization of Maml1, RAMIC, and Rbpj in nuclear foci in the presence of Aes and TLE1 (arrowheads). Scale bars, 10 μm.

(G) Effects of Aes and TLE1 on localization of Maml1 and transcription activity in the nucleus. HCT116 cells were transfected with expression plasmids for TLE1, Maml1, RAMIC and simultaneously with or without AcGFP-Aes and TLE1. Twenty-four hours later, the transfectants were pulse-labeled with BrUTP. Anti-BrUTP antibody localized newly synthesized mRNA in the nucleus. Note that Aes and Maml1 colocalized in the nuclear foci where few BrUTP speckles were observed

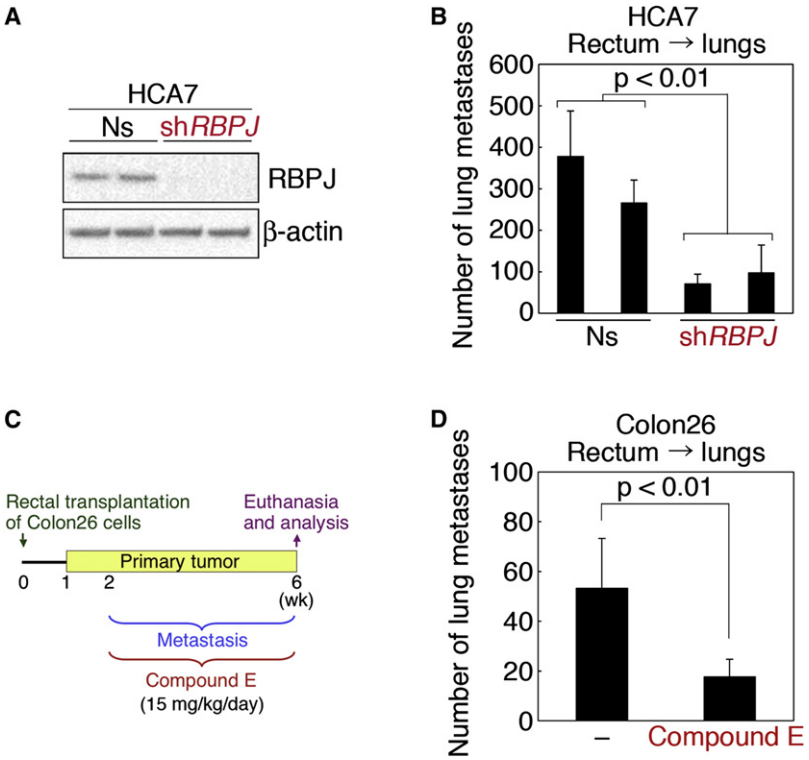

Figure 5. Suppression of Colon Cancer Metastasis by Inhibition of Notch Signaling

(A) Construction of HCA7 derivatives with constitutive expression of shRNA sequences against *RBPJ* mRNA (sh*RBPJ*), confirmed by western blotting. Clones were isolated using two different shRNAs. β-Actin is shown as a loading control. Ns, nonsilencing controls.

(B) Effects of sh*RBPJ* on lung metastasis of HCA7 derivatives transplanted into the nude mouse rectum. Error bars indicate SD (n = 10).

(C) Dosing scheme of Compound E for mice bearing Colon26 rectal tumors.

(D) Effects of Compound E on lung metastasis of Colon26 rectal tumors in Balb/c mice. –, Vehicle control. Data set shown is a representative of two. Error bars indicate SD (n = 8).

See also Figure S5.

called ''adenocarcinomas'' by histopathological definition, the extent of cellular atypia and epithelial architecture were rather similar to those in the $Apc^{\Delta 716}$ adenomas, without a very malignant appearance.

As in the transplantation results above (Figures S6A–S6C), blood vessels and macrophages expressed Dll4 ligand also in the *Apc/Aes* tumors (Figures 7H–7K). In addition, we found that smooth muscle layers as well as *muscularis mucosae* also expressed Dll4 ligand, although the invading tumor epithelium scarcely did (Figures 7L and 7M). Notably, the expression level of tumor *Hes1* was 1.5 times higher in *Apc/Aes* compound mutants than in *Apc* mutants (Figure 7N). Furthermore, treatment of the *Apc/Aes* mice with Compound E inhibited the tumor invasion significantly (Figure 7O), indicating a key role of Notch signaling in the invasion that was caused by *Aes* knockout. On the other hand, knocking out *Aes* did not affect the tumor size or number (Figure 7P).

DISCUSSION

In this study, we have demonstrated that *Aes* inhibits metastasis of colon cancer cells in an orthotopic transplantation model in mice. With conditional *Aes* knockout mutation in $Apc^{\Delta 716}$ polyposis mice, intestinal tumors showed local invasion and intravasation, two earliest steps in the metastatic cascade. These results indicate that inactivation of *Aes* accelerates local invasion and intra/extravasation, and plays critical roles in the metastatic spread of endogenous tumors. The invasion histopathology of the *Apc/Aes* mutants was distinctly different from that of the *cis-Apc/Smad4* adenocarcinomas. The latter tumors were surrounded by immature myeloid cells (iMCs; $CD34^{+}CD45^{+}CCR1^{+}$) and showed local invasion without intravasation (Kitamura et al., 2007; Kitamura and Taketo, 2007). In contrast, there were few iMCs around the invasion fronts of *Apc/Aes* tumors (data not shown), suggesting that tumors of these two models invade by different mechanisms.

Proliferation of Colon26 cells remained unaffected by *Aes* overexpression or knockdown, either in culture or upon grafting to the mouse rectum (Figures S2F–S2H; data not shown). Furthermore, the tumor number or size was not affected by the conditional *Aes* knockout (Figure 7P). Therefore, we conclude that *Aes* is an endogenous ''metastasis suppressor'' that inhibits metastasis but not tumorigenicity (Steeg, 2006; Smith and Theodorescu, 2009).

During the short life span of the *Apc/Aes* mutant mice (<18 weeks), we have been unable to find any overt metastasis in either liver or lungs. Because we initially used Colon26 cell line to find *Aes* gene downregulation in liver metastasis, we reasoned this difference from the *Apc/Aes* phenotype as below. First, the method of Colon26 injection into the rectal smooth muscle bypasses the local invasion, as well as intravasation

(arrowheads). On the other hand, in the absence of Aes, Maml1 distributed throughout the nucleoplasm where BrUTP was present (asterisks). Different from the top row photo, BrUTP-unstained area in AcGFP (bottom; marked as +) are also unstained for Maml1 in the left panel, suggesting that these areas are nucleoli rather than the foci. Scale bars, 10 μm.

(H) Colocalization of Aes and Rbpj on the nuclear matrix. HCT116 cells were transfected with expression plasmids for AcGFP or AcGFP-Aes simultaneously with TLE1, Rbpj, RAMIC, and Maml1. Twenty-four hours later, localization of the overexpressed proteins was analyzed by immunofluorescence (arrowheads in Whole cell). Note that AcGFP-Aes and Rbpj were retained inside the cells even after soluble proteins were washed off (arrowheads in Nuclear matrix). In contrast, Rbpj did not remain in the cells in the absence of Aes. Scale bars, 10 μm.

See also Figure S4.

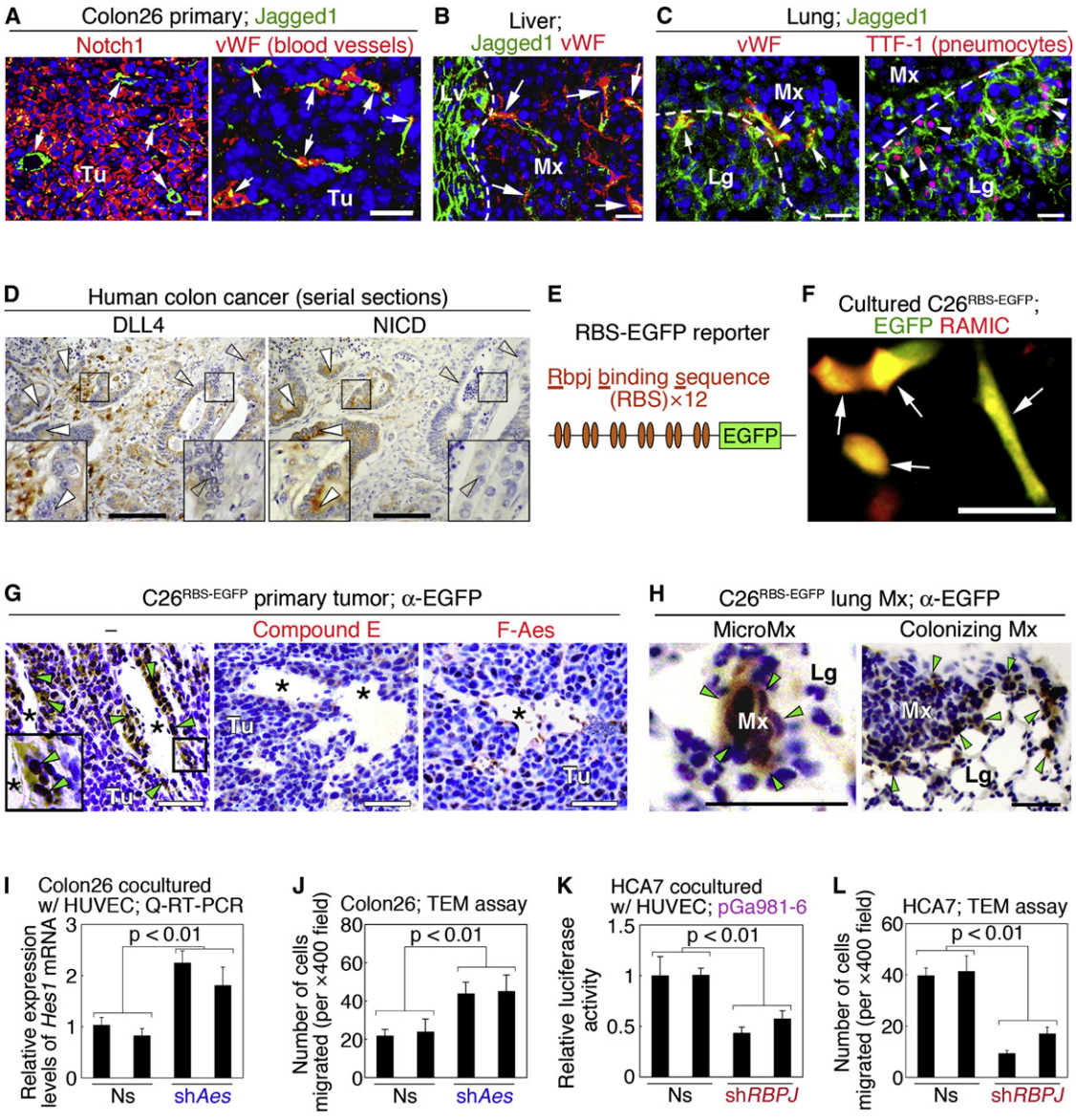

Figure 6. Activation of Notch Signaling in Cancer Cells by Adjoining Blood Endothelial Cells and Macrophages

(A) Immunofluorescence staining of Jagged1 (green) in a Colon26 tumor of the rectum. Red staining shows Notch1 (left) or blood vessel marker vWF (von Willebrand factor; right). DNA was stained with DAPI (blue). Arrows point representative Jagged1-expressing blood vessels. Tu, Tumor. Scale bars, 10 μm.

(B and C) Immunofluorescence staining of Jagged1 (green) in the liver (B) and lung (C) with Colon26 metastases. Red staining shows vWF, or Thyroid transcription factor (TTF) −1, a pneumocyte marker (C; right). Arrows and arrowheads point to the representative Jagged1-expressing blood vessels and pneumocytes adjoining the metastatic foci, respectively. Broken lines indicate the boundaries between the metastases and liver or lung tissues. Mx, metastasis. Lv and Lg, normal liver and lung tissues, respectively. DNA was stained with DAPI (blue). Scale bars, 10 μm.

(D) Close proximity of DLL4-expressing cells with NICD-expressing cells in human colon cancer. Serial sections were immunostained with anti-DLL4 (left) and anti-NICD (right) antibodies, respectively. Note that DLL4 was expressed in the stroma close to the cancer epithelium where NICD was stained (closed arrowheads in left insets). In contrast, cancer epithelium surrounded by DLL4-negative stroma showed little NICD staining (open arrowheads in right insets). Bars, 100 μm.

(E) A schematic representation of the RBS-EGFP reporter construct. The Notch signaling causes expression of EGFP through the tandem repeats of Rbpj binding sequence (RBS). The reporter was introduced into Colon26 cells to derive $C26^{RBS\text{-}EGFP}$ cells.

(F) Induction of EGFP in response to RAMIC expression in $C26^{RBS\text{-}EGFP}$ cells. An expression vector for myc-tagged RAMIC was transfected into the $C26^{RBS\text{-}EGFP}$ cells. Autofluorescence of EGFP and immunofluorescence signal of myc (red) were photographed under a fluorescence microscope, and merged electronically. Note that EGFP was induced in most of the RAMIC-expressing cells, merging as yellow (arrows). Scale bar, 10 μm.

(G and H) Activation of the Notch signaling within Colon26 primary tumors of the rectum (G, left) and its metastasis to the lung (H), detected by immunostaining for EGFP (green arrowheads). Boxed area in the left panel of (G) is enlarged in the inset. Note that treatment with Compound E (G, center) or overexpression of flag-tagged Aes (G, right) suppressed induction of EGFP. Asterisks, blood vessel lumens. Tu, tumor. Mx, metastasis. Lg, normal lung tissue. Scale bars, 50 μm.

because some fine vessels are destroyed upon injection. Second, Colon26 cells contain an activated *Kras* mutation allele. Accordingly, additional mutations in the *Apc*/*Aes* mutant mice may lead to overt metastasis of the intestinal tumors to distant organs.

Curiously, some of the cancer cells had already lost expression of *AES*/*Aes* on the invasion fronts in both human (Figure 1D, inset in the left panel) and mouse (Figure 1E) colon primary tumors. These results suggest that expression of *AES*/*Aes* is downregulated during the expansion of primary tumors. When cancer cells lose Aes, they can acquire the capacity to invade and intravasate. The mechanisms by which expression of Aes is downregulated remain to be investigated. We searched for *AES* mutations in colon cancer cell lines, without evidence so far. Although we tested the possibility of DNA methylation by treating colon cancer cell lines that lack AES with 5-aza-2-deoxycytidine, we found no increases in its expression. Thus, we speculate that *AES*/*Aes* gene is inactivated through some epigenetic changes other than DNA methylation.

Interestingly, we found that Aes colocalized with TLE1, Rbpj, RAMIC and Maml1 in nuclear foci where transcription is repressed (Figures 4D–4H). Because Aes is also associated and colocalized with HDAC3 in the foci (Figure S4), we speculate that Aes converts the transactivation complex to the MAD (matrix-associated deacetylase) bodies where HDAC proteins repress the Rbpj-dependent transcription (Kao et al., 1998; Downes et al., 2000). These results are consistent with reports that Notch repressors including SMRT and Mint/Sharp/Spen also show a similar speckled pattern in the nucleus (Kao et al., 1998; Downes et al., 2000; Oswald et al., 2002; Shi et al., 2001). Curiously, *Aes* null mice show a dwarf phenotype (Mallo et al., 1995, and data not shown). The dwarfism is caused by reduction in growth hormone-producing cells in the pituitary (Brinkmeier et al., 2003). Notably, the same dwarf phenotype is also reported in the transgenic mice overexpressing NICD, and in conditional knockout mice of the *Mint* gene (Zhu et al., 2006; Yabe et al., 2007), supporting the Notch-suppressing role of Aes in vivo.

It is possible that the elementary processes stimulated by Notch signaling are the motility and migration as implicated by our initial analysis of Aes in Matrigel (Figure S1G) and simpler scratch assays using recombinant Notch ligands (Figure S6F). Thus, we speculate that the enhanced motility contributes to TEM activity of cancer cells. It is conceivable that Notch signaling affects, either directly or indirectly, a series of small G proteins of the Rho family that can control the assembly of the actin cytoskeleton, as cell motility is regulated by such molecules (Weinberg, 2007). While these steps may be achieved by some carcinoma cells through a program of epithelial-mesenchymal transition (EMT), we have been unable to find signs of EMT in the Notch signaling-activated colon cancer or intestinal tumor cells. For example, tumor cells in the *Apc*/*Aes* compound mutants retained expression of cytokeratins and E-cadherin (Figures 7G–7I; data not shown) whose loss is a hallmark of EMT (Weinberg, 2007). Furthermore, expression of *Snail*, *Slug*, or *Twist* in Colon26 cells did not change upon transfection of *Aes* (data not shown). So far, about ten metastasis suppressor genes have been reported (Steeg, 2006; Smith and Theodorescu, 2009). Many of them appear to be involved in later steps in the metastasis cascade such as colonization, whereas some are involved in signal transduction pathways, including MAP kinase, Rho, Rac, and G protein-coupled and tyrosine kinase receptors. The effects of Aes downregulation in mutant mice on these genes remain to be investigated.

We found that Notch ligands Jagged1 and Dll4 were present on endothelial cells of the liver and lungs. Furthermore, we found ligand expression also on normal epithelium of the metastasis target organs (Figures 6B and 6C; Figures S6B and S6C). Convincingly, we found activated Notch signaling (expression of EGFP as a readout) in two types of metastasized cell clusters in the lung; micrometastases consisting of only a few cancer cells, and cells at the periphery of larger metastases that were expanding in the lung parenchyma (Figure 6H). Considering the fact that Aes can inhibit metastasis of cancer cells injected intravenously, we speculate that Aes also attenuates extravasation at the target organs. In addition, the ligand-expressing parenchymal cells adjoining the cancer cells may facilitate the metastatic expansion through stimulation of cancer invasion into the surrounding tissues, and inhibition of apoptosis in cancer cells (Artavanis-Tsakonas et al., 1999).

By searching the ONCOMINE database (http://www.oncomine.org/), we found that data were compiled showing the correlation between *AES* downregulation and metastasis for a variety of cancers such as prostate, bladder, breast, and ovarian cancers, and sarcoma, neuroblastoma, etc. These data suggest that *AES* has a metastasis-suppressing role also in other types of cancer. Furthermore, these results imply that earlier steps of the invasion-metastasis cascade are probably similar in various types of human tumors, although the last step—colonization—is likely to depend on complex interactions between the metastasizing cells and microenvironments of the host tissues where they land (Weinberg, 2007).

In summary, we have demonstrated that *Aes* is a metastasis suppressor that prevents local tumor invasion and intravasation through inhibition of Notch signaling. When cancer cells retain expression of *Aes*, it suppresses Notch signaling that is triggered

(I) Effects of *Aes* knockdown by shRNA against *Aes* mRNA (sh*Aes*) on Notch signaling. Colon26 cells with (sh*Aes*) or without (Ns; nonsilencing) constitutive expression of sh*Aes* were cocultured with HUVEC. Twelve hours later, cells were harvested and expression of mouse *Hes1* mRNA was quantified. Error bars indicate SD (n = 3).
(J) Effects of sh*Aes* on transendothelial migration (TEM) of Colon26 cells. Twenty-four hours after coculture, Colon26 cells that had migrated through the HUVEC layer were counted. Error bars indicate SD (n = 3).
(K) Effects of shRNA against *RBPJ* mRNA (sh*RBPJ*) on Notch signaling. Two independent HCA7 clones were derived by introducing nonsilencing control (Ns) and *RBPJ* knockdown (sh*RBPJ*) constructs, respectively, and transfected with the luciferase reporter followed by coculture with HUVEC. At 12 hr posttransfection, luciferase activity was determined. Error bars indicate SD (n = 3).
(L) Effects of sh*RBPJ* on TEM activity of HCA7 cancer cells. HCA7 cells were placed on a layer of HUVEC. Twenty-four hours later, HCA7 cells were counted that had migrated through the HUVEC layer. Error bars in (I–L) indicate SD of three independent experiments.
See also Figure S6 and Movie S1.

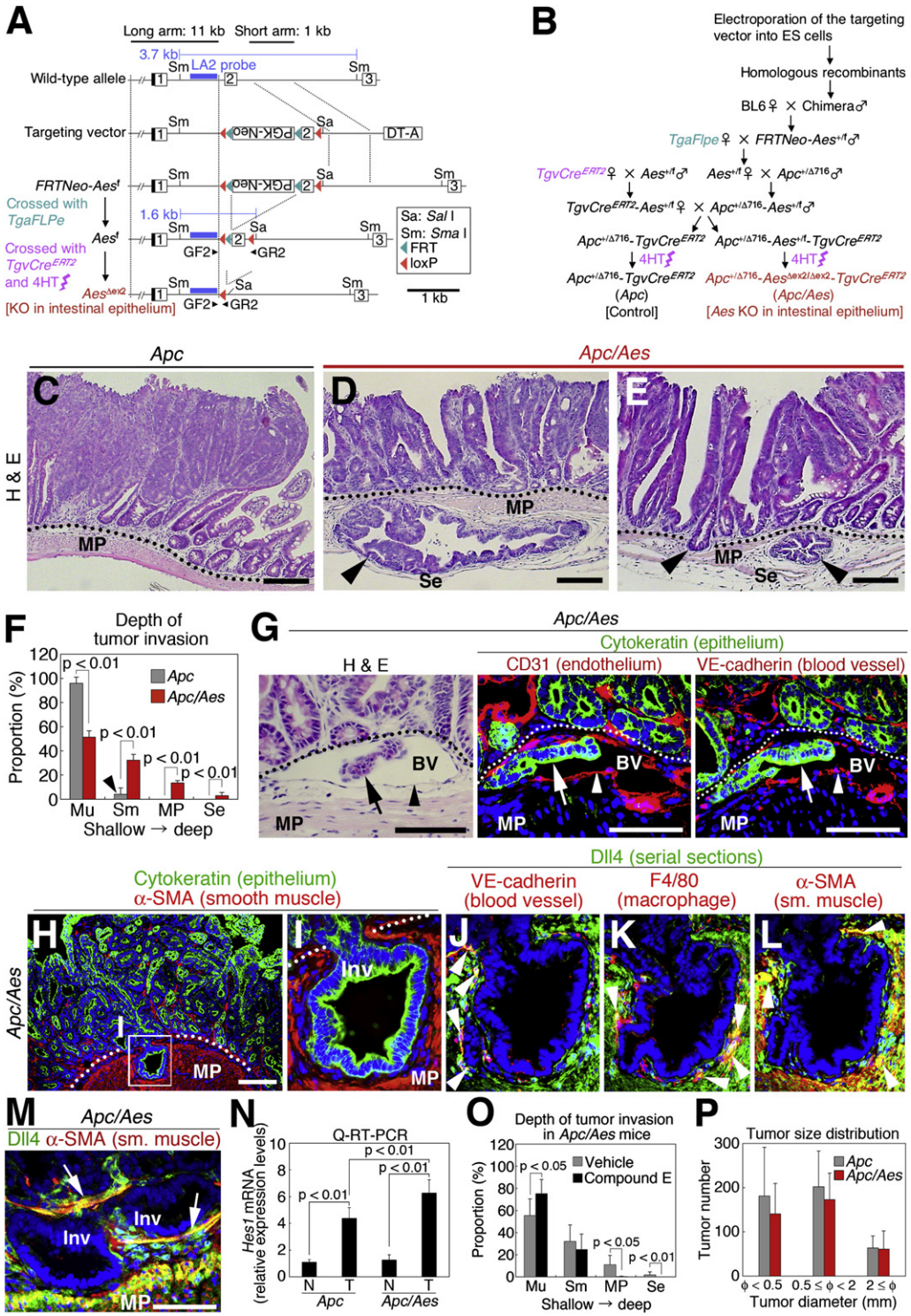

Figure 7. Local Tumor Invasion and Intravasation Phenotypes of the Compound Knockout Mice for *Aes* and *Apc* Genes

(A) Targeting strategy for the *Aes* allele specifically in the intestinal epithelium. Restriction sites and a Southern blotting probe are shown. PCR primers GF2 and GR2 were used to distinguish the floxed allele (Aes^{f}) from the targeted allele ($Aes^{\Delta ex2}$) of *Aes* gene after Cre activation by 4-hydroxytamoxifen (4HT).

(B) Breeding scheme for generating $Apc^{+/\Delta 716}$-$Aes^{f/f}$-$TgvCre^{ERT2}$ compound mutants. Germline mice with the targeted *Aes* allele flanked by a PGK-Neo cassette (*FRTNeo-Aes*$^{+/f}$) were crossed with a transgenic strain where expression of Flpe was driven by actin promoter (*TgaFlpe*) to remove the cassette. Resulting $Aes^{+/f}$ mice were crossed with another transgenic strain carrying an expression cassette for Cre^{ERT2} driven by villin promoter (*TgvCre*^{ERT2}) and *Apc* knockout mice ($Apc^{+/\Delta 716}$), to generate $Apc^{+/\Delta 716}$-$Aes^{f/f}$-$TgvCre^{ERT2}$ compound mutant mice. Treating them with 4HT activated Cre^{ERT2}, knocking out the *Aes* gene (*Apc/Aes*).

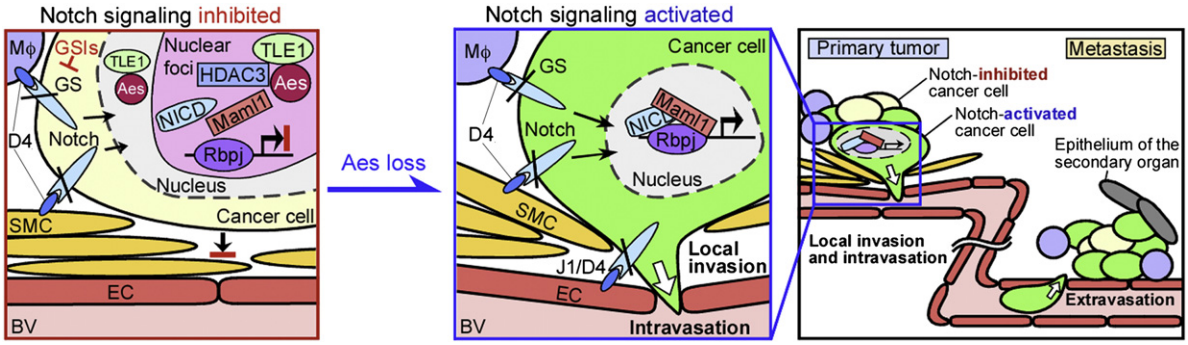

Figure 8. A Schematic Representation of Aes as a Notch Signaling Inhibitor, Hence a Metastasis Suppressor

When Notch receptor on a cancer cell is bound by Dll4 (D4) or Jagged1 (J1) ligand on adjoining macrophages (Mϕ), smooth muscle cells (SMC), or endothelial cells (EC), Notch intracellular domain (NICD) is released by γ-secretase (GS) cleavage. We propose that Aes relocates to nuclear foci with TLE1, Rbpj, NICD, Maml1, and HDAC3, to repress transcription (left). Once Aes is lost in a cancer cell, the transcription is derepressed, stimulating its local invasion and intravasation into the blood vessel (BV, center). In addition, Notch signaling is likely to promote extravasation of the cancer cell at the target organ, enhancing its metastasis (right). GSIs, GS inhibitors.

by the stromal cells (Figure 8, left). Once cancer cells lose its expression, derepressed Notch signaling can stimulate their local invasion (Figure 8, center), enhancing intravasation to promote metastasis (Figure 8, right). Because numerous compounds and biologicals have been evaluated as Notch signaling inhibitors, it is possible that some of such agents prove clinically efficacious in the treatment and prevention of cancer metastasis.

EXPERIMENTAL PROCEDURES

Animals

Balb/c, C57BL/6, and nude mice were purchased from CLEA (Japan). *Apc*$^{\Delta 716}$ and *TgvCre*^{ERT2} mice have been described previously (Oshima et al., 1995; el Marjou et al., 2004). *TgaFlpe* mice were obtained from the Jackson Laboratory. All animal experiments were conducted according to the protocol approved by the Animal Care and Use Committee of Kyoto University.

Microarray Analysis

RNA samples were prepared from Colon26 cells in primary tumors and their liver metastases using TRI reagent (SIGMA). Gene expression profiles were analyzed using 3D-Gene Mouse Oligo Chip 24k (TORAY).

Clinical Samples

Cancer tissues had been resected from patients who had undergone operations with informed consents, with the protocol approved by the Ethics Committee of Kyoto University or Kitano Hospital. Tumors were fixed by formalin and embedded in paraffin wax.

Conditional Knockout of *Aes* Allele

As shown in Figure 7A, we constructed a targeting vector where the PGK-Neo cassette sandwiched with FRT sequences was inserted into intron 1 immediately 5′ to exon 2 of *Aes*, followed by addition of loxP sequences sandwiching the insert and exon 2. The vector was constructed using the recombineering technology (Liu et al., 2003). A BAC clone bMQ-222K13 containing whole *Aes* gene of 129 strain was obtained from Geneservice (UK). A 13 kb DNA fragment spanning from 8 kb upstream of exon 1 to 2 kb downstream of exon 2 was retrieved from the BAC, and subcloned into pMCS-DTA vector to construct "pMCS-DTA-Aes" using SW102 strain of *Escherichia coli*. A PGK-Neo cassette sandwiched with two loxP sequences was excised from PL452 plasmid and inserted at downstream of exon 2 in pMCS-DTA-Aes to construct "pMCS-DTA-loxNeo-Aes." After induction of Cre recombinase by arabinose in SW106 strain of *E.coli*, the pMCS-DTA-loxNeo-Aes was introduced into the SW106. Upon Cre-mediated excision of the PGK-Neo cassette, one loxP sequence was left at downstream of exon 2, creating "pMCS-DTA-lox-Aes." Then a PGK-Neo cassette sandwiched with two FRT

(C–E) Histopathology of the small intestine at 17 weeks of age (H & E). In the control (*Apc*), adenoma cells remained above the *muscularis mucosae* (dotted line; C). In the *Apc/Aes* compound mutant mice, tumor cells invaded the *muscularis mucosae* and *muscularis propria* (MP), reaching the *serosa* (Se) (arrowheads in D and E). Scale bars, 100 μm.

(F) Quantification of the depth of tumor invasion in the small intestine at 17 weeks of age. Note that the tumor cells in the compound mutants (*Apc/Aes*; red) but not controls (*Apc*; gray) deeply invaded into the *submucosa* (Sm). Mu, *mucosa*. MP, *muscularis propria*. Se, *serosa*. Arrowhead, pseudoinvasion (herniation) in *Apc* control. n = 5 for each group.

(G) Tumor intravasation in the *Apc/Aes* mice. Left, An H&E staining suggested tumor cells (arrow) inside a blood vessel (BV; also indicated by arrowhead) near the *muscularis mucosae* (dotted line). This interpretation was verified by immunofluorescence in the adjoining sections for epithelial marker cytokeratin (green; arrow), and vessel marker CD31 (red; center) as well as blood vessel marker VE-cadherin (right). MP, *muscularis propria*. Scale bars, 50 μm.

(H–L) Expression of Dll4 ligand on stromal cells analyzed by immunostaining of serial sections. Epithelial cells express cytokeratin (green), whereas smooth muscle cells (MP; *muscularis propria*) express α-smooth muscle actin (α-SMA in red; H). Boxed area in (H) is enlarged in (I), whose serial sections are (J), (K), and (L). Blood vessels (stained for VE-cadherin in red; J), macrophages (F4/80 in red; K), and smooth muscle (α-SMA in red; L) expressed Dll4 (green) merging as yellow (arrowheads) around the local invasion of tumor epithelium. Scale bar, 100 μm.

(M) Immunofluorescence of Dll4 (green) and α-SMA (red) in the invading tumor of the *Apc/Aes* mutant (Inv). Note that smooth muscle cells in the *muscularis mucosae* (arrows) as well as the *muscularis propria* (MP) expressed Dll4 ligand. Scale bar, 50 μm.

(N) Expression levels of *Hes1* mRNA in the mouse small intestine determined by Q-RT-PCR. N, normal mucosa. T, tumor. Error bars indicate SD (n = 5).

(O) Effects of Compound E on depth of tumor invasion. *Apc/Aes* mice were treated with (black bars) or without (gray bars) Compound E for 10 weeks. Error bars indicate SD (n = 5 for each group).

(P) Size distribution of tumors in the small intestine at 17 weeks of age. Control *Apc* is shown in gray, whereas *Apc/Aes* is indicated in red. Error bars indicate SD (n = 5).

See also Figure S7.

sequences followed by a loxP sequence was excised from PL451 plasmid (NCI), and inserted upstream of exon 2, generating the targeting vector "pMCS-DTA-FRTNeo-Aes^{f}" (Figure 7A). The integrity of the construct was verified by PCR and restriction digestion after introduction of the vector into Cre-expressing SW106 or Flpe-expressing SW105 strains (NCI). Then, the vector was introduced into D3a2 ES cells by homologous recombination and targeted ES clones were selected and karyotyped. Germ line-transmitted mice (*FRTNeo-Aes*$^{+/f}$) were generated and the PGK-Neo selection sequence was removed by crossing with actin promoter-driven FLPe transgenic mice (*TgaFlpe*) (Jackson Laboratory, ME), producing mice with a floxed *Aes* allele (*Aes*$^{+/f}$) (Figure S7B). We verified that homozygotes of these floxed *Aes* wild-types are viable, fertile and without any obvious phenotypes (data not shown). As shown in Figure 7B, we then crossed these *Aes*$^{+/f}$ female mice with *Apc*$^{+/\Delta716}$ males, and further crossed their compound heterozygotes with the compound heterozygotes obtained from crosses between *Aes*$^{+/f}$ males and Villin-Cre^{ERT2} transgenic (*TgvCre*^{ERT2}) females. At 3 weeks of age, the progeny compound mutant mice (*Apc*$^{+/\Delta716}$-*Aes*$^{f/f}$-*TgvCre*^{ERT2}) were treated with 4-hydroxytamoxifen (4HT; SIGMA) to activate Cre recombinase in the intestine-specific manner (el Marjou et al., 2004), generating *Apc*$^{+/\Delta716}$-*Aes*$^{\Delta ex2/\Delta ex2}$-*TgvCre*^{ERT2}, abbreviated as *Apc/Aes*.

Data Analysis

Data were analyzed by Student's t or chi-square tests and are presented as mean ± SD. P values <0.05 were considered significant.

ACCESSION NUMBERS

Microarray hybridization data have been deposited in the GEO database with accession code GSE12162.

SUPPLEMENTAL INFORMATION

Supplemental Information includes Supplemental Experimental Procedures, seven figures, and two movies and can be found with this article online at doi:10.1016/j.ccr.2010.11.008.

ACKNOWLEDGMENTS

We thank H. Kikuchi and Y. Mouri for excellent technical assistance, T. Honjo for plasmids and suggestions, T. Sudo for microarray analyses, Y. Yui and T. Tanaka for time-lapse microphotography, O. Takahashi for high-magnification fluorescence microphotography, S. Stifani for anti-panTLE antibody, H. Sasaki for Hedgehog reporters, T. Ishikawa, H. Miyoshi, A. Deguchi, S. Arimura, S. Yamashita, I. Okazaki, T. Okazaki, K. Okawa, C. Takahashi, T. Tomita, and Y. Morohashi for helpful discussions, S. Takahashi for microinjection of ES cells into blastcysts, N. Copeland, N. Jenkins, J. Takeda, and K. Yusa for biologicals and suggestions for the recombineering system. We also thank P. Vogt, To. Kitamura, M. Okabe, M. Kitagawa, and S. Kirkland for providing vectors pBSfi-AU1-TLE1, pMX-IRES-EGFP, pCX, Maml1 cDNA and HCA7 cells, respectively. This work was supported by grants from Ministry of Education, Culture, Sports, Science and Technology (MEXT), Japan, and by Jeannik M. Littlefield-AACR Grant in Metastatic Colon Cancer Research.

Received: June 7, 2010
Revised: September 17, 2010
Accepted: November 2, 2010
Published: January 18, 2011

REFERENCES

Artavanis-Tsakonas, S., Rand, M.D., and Lake, R.J. (1999). Notch signaling: cell fate control and signal integration in development. Science *284*, 770–776.

Brantjes, H., Roose, J., van de Wetering, M., and Clevers, H. (2001). All Tcf HMG box transcription factors interact with Groucho-related co-repressors. Nucleic Acids Res. *29*, 1410–1419.

Brinkmeier, M.L., Potok, M.A., Cha, K.B., Gridley, T., Stifani, S., Meeldijk, J., Clevers, H., and Camber, S.A. (2003). TCF and Groucho-related genes influence pituitary growth and development. Mol. Endocrinol. *17*, 2152–2161.

Chen, G., and Courey, A.J. (2000). Groucho/TLE family proteins and transcriptional repression. Gene *249*, 1–16.

Christofori, G. (2006). New signals from the invasive front. Nature *441*, 444–450.

Corbett, T.H., Griswold, D.P., Jr., Roberts, B.J., Peckham, J.C., and Schabel, F.M., Jr. (1975). Tumor induction relationships in development of transplantable cancers of the colon in mice for chemotherapy assays, with a note on carcinogen structure. Cancer Res. *35*, 2434–2439.

Detre, S., Saclani Jotti, G., and Dowsett, M. (1995). A "quickscore" method for immunohistochemical semiquantitation: validation for oestrogen receptor in breast carcinomas. J. Clin. Pathol. *48*, 876–878.

Downes, M., Ordentlich, P., Kao, H.-Y., Alvarez, J.G.A., and Evans, R.M. (2000). Identification of a nuclear domain with deacetylase activity. Proc. Natl. Acad. Sci. USA *97*, 10330–10335.

el Marjou, F., Janssen, K.P., Chang, B.H., Li, M., Hindie, V., Chan, L., Louvard, D., Chambon, P., Metzger, D., and Robine, S. (2004). Tissue-specific and inducible Cre-mediated recombination in the gut epithelium. Genesis *39*, 186–193.

Fidler, I.J. (2003). The pathogenesis of cancer metastasis: the "seed and soli" hypothesis revisited. Nat. Rev. Cancer *3*, 453–458.

Gasperowicz, M., and Otto, F. (2005). Mammalian Groucho homologs: redundancy or specificity? J. Cell. Biochem. *95*, 670–687.

Hoshino, H., Nishino, T.G., Tashiro, S., Miyazaki, M., Ohmiya, Y., Igarashi, K., Horinouchi, S., and Yoshida, M. (2007). Co-repressor SMRT and class II histone deacetylase promote Bach2 nuclear retention and formation of nuclear foci that are responsible for local transcriptional repression. J. Biochem. *141*, 719–727.

Hurlbut, G.D., Kankel, M.W., Lake, R.J., and Artavanis-Tsakonas, S. (2007). Crossing paths with Notch in the hyper-network. Curr. Opin. Cell Biol. *19*, 166–175.

Ilagan, M.X., and Kopan, R. (2007). Snapshot: Notch signaling pathway. Cell *128*, 1246.

Kao, H.Y., Ordentlich, P., Koyano-Nakagawa, N., Tang, Z., Downes, M., Kintner, C.R., Evans, R.M., and Kadesch, T. (1998). A histone deacetylase corepressor complex regulates the Notch signal transduction pathway. Genes Dev. *12*, 2269–2277.

Kashtan, H., Rabau, M., Mullen, J.B.M., Wong, A.H.C., Roder, J.C., Shpitz, B., Stern, H.S., and Gallinger, S. (1992). Intra-rectal injection of tumor cells: a novel animal model of rectal cancer. Surg. Oncol. *1*, 251–256.

Kato, H., Taniguchi, Y., Kurooka, H., Minoguchi, S., Sakai, T., Nomura-Okazaki, S., Tamura, K., and Honjo, T. (1997). Involvement of RBP-J in biological functions of mouse Notch1 and its derivatives. Development *124*, 4133–4141.

Kirkland, S.C. (1985). Dome formation by human colonic adenocarcinoma cell line (HCA-7). Cancer Res. *45*, 3790–3795.

Kitamura, T., and Taketo, M.M. (2007). Keeping out the bad guys: gateway to cellular target therapy. Cancer Res. *67*, 10099–10102.

Kitamura, T., Kometani, K., Hashida, H., Matsunaga, A., Miyoshi, H., Hosogi, H., Aoki, M., Oshima, M., Hattori, M., Takabayashi, A., et al. (2007). SMAD4-deficient intestinal tumors recruit CCR1^{+} myeloid cells that promote invasion. Nat. Genet. *39*, 467–475.

Lepourcelet, M., and Shivdasani, R.A. (2002). Characterization of a novel mammalian Groucho isoform and its role in transcriptional regulation. J. Biol. Chem. *277*, 47732–47740.

Liu, P., Jenkins, N.A., and Copeland, N.G. (2003). A highly efficient recombineering-based method for generating conditional knockout mutations. Genome Res. *13*, 476–484.

Lu, C., Bonome, T., Li, Y., Kmat, A.A., Han, L.Y., Schmandt, R., Coleman, R.L., Gershenson, D.M., Jaffe, R.B., Birrer, M.J., et al. (2007). Gene alterations identified by expression profiling in tumor-associated endothelial cells from invasive ovarian carcinoma. Cancer Res. *67*, 1757–1768.

Mailhos, C., Modlich, U., Lewis, J., Harris, A., Bicknell, R., and Ish-Horowicz, D. (2001). Delta4, an endothelial specific notch ligand expressed at sites of physiological and tumor angiogenesis. Differentiation *69*, 135–144.

Mallo, M., Gendron-Maguire, M., Harbison, M.L., and Gridley, T. (1995). Protein characterization and targeted disruption of *Grg*, a mouse gene related to the *groucho* transcript of the *Drosophila Enhancer of split* complex. Dev. Dyn. *204*, 338–347.

Milano, J., McKay, J., Dagenais, C., Foster-Brown, L., Pognan, F., Gadient, R., Jacobs, R.T., Zacco, A., Greenberg, B., and Ciaccio, P.J. (2004). Modulation of Notch processing by γ-secretase inhibitors causes intestinal goblet cell metaplasia and induction of genes known to specify gut secretory lineage differentiation. Toxicol. Sci. *82*, 341–358.

Oshima, M., Oshima, H., Kitagawa, K., Kobayashi, M., Itakura, C., and Taketo, M. (1995). Loss of *Apc* heterozygosity and abnormal tissue building in nascent intestinal polyps in mice carrying a truncated *Apc* gene. Proc. Natl. Acad. Sci. USA *92*, 4482–4486.

Oswald, F., Kostezka, U., Astrahantseff, K., Bourteele, S., Dillinger, K., Zechner, U., Ludwig, L., Wilda, M., Hameister, H., Knöchel, W., et al. (2002). SHARP is a novel component of the Notch/RBP-Jκ signalling pathway. EMBO J. *21*, 5417–5426.

Pinto, M., and Lobe, C.G. (1996). Products of the *grg* (*Groucho-related gene*) family can dimerize through the amino-terminal Q domain. J. Biol. Chem. *271*, 33026–33031.

Price, J.E. (2001). Xenograft models in immunodeficient animals: I. nude mice. In Methods in molecular medicine: Metastasis research protocols, *Volume II*, S.A. Brooks and U. Schumacher, eds. (Totowa, NJ: Humana Press), pp. 205–214.

Roose, J., Molenaar, M., Peterson, J., Kurenkamp, J., Brantjes, H., Moerer, P., van de Wetering, M., Destree, O., and Clevers, H. (1998). The *Xenopus* Wnt effector XTcf-3 interacts with Groucho-related transcriptional repressors. Nature *395*, 608–612.

Sancho, E., Batlle, E., and Clevers, H. (2004). Signaling pathways in intestinal development and cancer. Annu. Rev. Cell Dev. Biol. *20*, 695–723.

Schmidt, B. (2003). Aspartic proteases involved in Alzheimer's disease. ChemBioChem *4*, 366–378.

Shi, Y., Downes, M., Xie, W., Kao, H.Y., Ordentlich, P., Tsai, C.C., Hon, M., and Evans, R.M. (2001). Sharp, an inducible cofactor that integrates nuclear receptor repression and activation. Genes Dev. *15*, 1140–1151.

Smith, S.C., and Theodorescu, D. (2009). Learning therapeutic lessons from metastasis suppressor proteins. Nat. Rev. Cancer *9*, 253–264.

Steeg, P.S. (2006). Tumor metastasis: mechanistic insights and clinical challenges. Nat. Med. *12*, 895–904.

Takaku, K., Oshima, M., Miyoshi, H., Matsui, M., Seldin, M.F., and Taketo, M.M. (1998). Intestinal tumorigenesis in compound mutant mice of both *Dpc4* (*Smad4*) and *Apc* genes. Cell *92*, 645–656.

Taketo, M.M. (2006). Wnt signaling and gastrointestinal tumorigenesis in mouse models. Oncogene *25*, 7522–7530.

Taketo, M.M., and Edelman, W. (2009). Mouse models of colon cancer. Gastroenterology *136*, 780–798.

Tsutsumi, S., Kuwano, H., Morinaga, N., Shimura, T., and Asao, T. (2001). Animal model of para-aortic lymph node metastasis. Cancer Lett. *169*, 77–85.

van Es, J.H., Jay, P., Gregorieff, A., van Gijn, M.E., Jonkheer, S., Hatzis, P., Thiel, T.J., van den Born, M., Begthel, H., Brabletz, T., et al. (2005). Wnt signaling induces maturation of Paneth cells in intestinal crypts. Nat. Cell Biol. *7*, 381–386.

Wang, W.F., Wang, Y.G., Reginato, A.M., Plotkina, S., Gridley, T., and Olsen, B.R. (2002). Growth defect in Grg5 null mice is associated with reduced Ihh signaling in growth plates. Dev. Dyn. *224*, 79–89.

Weinberg, R.A. (2007). Moving out: invasion and metastasis. In The Biology of Cancer (New York: Garland Science), pp. 587–654.

Yabe, D., Fukuda, H., Aoki, M., Yamada, S., Takebayashi, S., Shinkura, R., Yamamoto, N., and Honjo, T. (2007). Generation of a conditional knockout allele for mammalian Spen protein Mint/SHARP. Genesis *45*, 300–306.

Zaczek, R., Olson, R.E., Seiffert, D.A., and Thompson, L.A. (1999). Compounds for inhibiting beta-amyloid peptide release and/or its synthesis. PCT Int. Appl. WO99/67221.

Zagouras, P., Stifani, S., Blaumueller, C.M., Carcangiu, M.L., and Artavanis-Tsakonas, S. (1995). Alterations in Notch signaling in neoplastic lesions of the human cervix. Proc. Natl. Acad. Sci. USA *92*, 6414–6418.

Zhu, X., Zhang, J., Tollkuhn, J., Ohsawa, R., Bresnick, E.H., Guillemot, F., Kageyama, R., and Rosenfeld, M. (2006). Sustained Notch signaling in progenitors is required for sequential emergence of distinct cell lineages during organogenesis. Genes Dev. *20*, 2739–2753.

Zimber, A., Nguyen, Q.D., and Gespach, C. (2004). Nuclear bodies and compartments: functional roles and cellular signaling in health and disease. Cell. Signal. *16*, 1085–1104.